Research Article | Vol. 25, No. 13 | 26 Jun 2017 | OPTICS EXPRESS 14173

Optics EXPRESS

Polymer X-ray refractive nano-lenses fabricated by additive technology

A. K. Petrov,[1,2] V. O. Bessonov,[1] K. A. Abrashitova,[1] N. G. Kokareva,[1] K. R. Safronov,[1] A. A. Barannikov,[2] P. A. Ershov,[2] N. B. Klimova,[2] I. I. Lyatun,[2] V. A. Yunkin,[3] M. Polikarpov,[2] I. Snigireva,[4,*] A. A. Fedyanin,[1] and A. Snigirev[2]

[1]*Faculty of Physics, Lomonosov Moscow State University, 1 Leninskie Gory, 119991 Moscow, Russia*
[2]*Immanuel Kant Baltic Federal University, 14 Nevskogo, 236041 Kaliningrad, Russia*
[3]*Institute of Microelectronics Technology RAS, Chernogolovka, Russia*
[4]*European Synchrotron Radiation Facility, 71 avenue des Martyrs, Grenoble, 38043, France*
**irina@esrf.fr*

Abstract: The present work demonstrates the potential applicability of additive manufacturing to X-Ray refractive nano-lenses. A compound refractive lens with a radius of 5 µm was produced by the two-photon polymerization induced lithography. It was successfully tested at the X-ray microfocus laboratory source and a focal spot of 5 µm was measured. An amorphous nature of polymer material combined with the potential of additive technologies may result in a significantly enhanced focusing performance compared to the best examples of modern X-ray compound refractive lenses.

OCIS codes: (000.2700) General science; (180.7460) X-ray microscopy; (340.7440) X-ray imaging; (350.3950) Micro-optics.

References and links

1. A. Snigirev, V. Kohn, I. Snigireva, and B. Lengeler, "A compound refractive lens for focusing high-energy x-rays," Nature **384**(6604), 49–51 (1996).
2. A. Snigirev, I. Snigireva, M. Grigoriev, V. Yunkin, M. Di Michiel, S. Kuznetsov, and G. Vaughan, "Silicon planar lenses for high energy x-ray nanofocusing," Proc. SPIE **6705**, 670506 (2007).
3. B. Lengeler, C. Schroer, J. Tümmler, B. Benner, M. Richwin, A. Snigirev, I. Snigireva, and M. Drakopoulos, "Imaging by parabolic refractive lenses in the hard x-ray range," J. Synchrotron Radiat. **6**(6), 1153–1167 (1999).
4. B. Lengeler, C. G. Schroer, M. Kuhlmann, B. Benner, T. F. Günzler, O. Kurapova, F. Zontone, A. Snigirev, and I. Snigireva, "Refractive x-ray lenses," J. Phys. D Appl. Phys. **38**(10A), A218–A222 (2005).
5. V. Aristov, M. Grigoriev, S. Kuznetsov, L. Shabelnikov, V. Yunkin, T. Weitkamp, C. Rau, I. Snigireva, A. Snigirev, M. Hoffmann, and E. Voges, "X-ray refractive planar lens with minimized absorption," Appl. Phys. Lett. **77**(24), 4058–4060 (2000).
6. M. Polikarpov, I. Snigireva, J. Morse, V. Yunkin, S. Kuznetsov, and A. Snigirev, "Large-acceptance diamond planar refractive lenses manufactured by laser cutting," J. Synchrotron Radiat. **22**(1), 23–28 (2015).
7. S. Terentyev, V. Blank, S. Polyakov, S. Zholudev, A. Snigirev, M. Polikarpov, T. Kolodziej, J. Qian, H. Zhou, and Y. Shvyd'ko, "Parabolic single-crystal diamond lenses for coherent x-ray imaging," Appl. Phys. Lett. **107**(11), 111108 (2015).
8. S. Terentyev, M. Polikarpov, I. Snigireva, M. Di Michiel, S. Zholudev, V. Yunkin, S. Kuznetsov, V. Blank, and A. Snigirev, "Linear parabolic single-crystal diamond refractive lenses for synchrotron x-ray sources," J. Synchrotron Radiat. **24**(1), 103–109 (2017).
9. A. Snigirev, I. Snigireva, G. Vaughan, J. Wright, M. Rossat, A. Bytchkov, and C. Curfs, "High energy x-ray transfocator based on al parabolic refractive lenses for focusing and collimation," J. Phys. Conf. Ser. **186**, 012073 (2009).
10. G. B. Vaughan, J. P. Wright, A. Bytchkov, M. Rossat, H. Gleyzolle, I. Snigireva, and A. Snigirev, "X-ray transfocators: Focusing devices based on compound refractive lenses," J. Synchrotron Radiat. **18**(2), 125–133 (2011).
11. P. Ershov, S. Kuznetsov, I. Snigireva, V. Yunkin, A. Goikhman, and A. Snigirev, "Fourier crystal diffractometry based on refractive optics," J. Appl. Cryst. **46**(5), 1475–1480 (2013).
12. M. Drakopoulos, A. Snigirev, I. Snigireva, and J. Schilling, "X-ray high-resolution diffraction using refractive lenses," Appl. Phys. Lett. **86**(1), 014102 (2005).
13. A. Bosak, I. Snigireva, K. S. Napolskii, and A. Snigirev, "High-resolution transmission x-ray microscopy: A new tool for mesoscopic materials," Adv. Mater. **22**(30), 3256–3259 (2010).

#292676 https://doi.org/10.1364/OE.25.014173
Journal © 2017 Received 17 Apr 2017; revised 21 May 2017; accepted 21 May 2017; published 13 Jun 2017

Optics EXPRESS

14. D. V. Byelov, J. Hilhorst, A. B. G. M. Leferink op Reinink, I. Snigireva, A. Snigirev, G. B. M. Vaughan, G. Portale, and A. V. Petukhov, "Diffuse scattering in random-stacking hexagonal close-packed crystals of colloidal hard spheres," Phase Transit. **83**(2), 107–114 (2010).
15. B. Lengeler, C. G. Schroer, M. Richwin, J. Tümmler, M. Drakopoulos, A. Snigirev, and I. Snigireva, "A microscope for hard x rays based on parabolic compound refractive lenses," Appl. Phys. Lett. **74**(26), 3924–3926 (1999).
16. H. Simons, A. King, W. Ludwig, C. Detlefs, W. Pantleon, S. Schmidt, I. Snigireva, A. Snigirev, and H. F. Poulsen, "Dark-field x-ray microscopy for multiscale structural characterization," Nat. Commun. **6**, 6098 (2015).
17. I. Snigireva, G. B. M. Vaughan, A. Snigirev, I. McNulty, C. Eyberger, and B. Lai, "High-energy nanoscale-resolution x-ray microscopy based on refractive optics on a long beamline," AIP Conf. Proc. **1365**, 188–191 (2011).
18. V. Kohn, I. Snigireva, and A. Snigirev, "Diffraction theory of imaging with x-ray compound refractive lens," Opt. Commun. **216**(4-6), 247–260 (2003).
19. A. Snigirev, I. Snigireva, M. Lyubomirskiy, V. Kohn, V. Yunkin, and S. Kuznetsov, "X-ray multilens interferometer based on si refractive lenses," Opt. Express **22**(21), 25842–25852 (2014).
20. C. G. Schroer, O. Kurapova, J. Patommel, P. Boye, J. Feldkamp, B. Lengeler, M. Burghammer, C. Riekel, and L. Vincze, "Hard x-ray nanoprobe with refractive x-ray lenses," Acta Crystallogr. A **62**(a1), s93 (2006).
21. C. G. Schroer and B. Lengeler, "Focusing hard x rays to nanometer dimensions by adiabatically focusing lenses," Phys. Rev. Lett. **94**(5), 054802 (2005).
22. A. I. Kuznetsov, R. Kiyan, and B. N. Chichkov, "Laser fabrication of 2d and 3d metal nanoparticle structures and arrays," Opt. Express **18**(20), 21198–21203 (2010).
23. I. Utke, P. Hoffmann, and J. Melngailis, "Gas-assisted focused electron beam and ion beam processing and fabrication," J. Vac. Sci. Technol. B Microelectron. Nanometer Struct. Process. Meas. Phenom. **26**(4), 1197 (2008).
24. Y.-Y. Cao, N. Takeyasu, T. Tanaka, X.-M. Duan, and S. Kawata, "3d metallic nanostructure fabrication by surfactant-assisted multiphoton-induced reduction," Small **5**(10), 1144–1148 (2009).
25. C. Sun, N. Fang, D. M. Wu, and X. Zhang, "Projection micro-stereolithography using digital micro-mirror dynamic mask," Sens. Actuators A Phys. **121**(1), 113–120 (2005).
26. S. Maruo, O. Nakamura, and S. Kawata, "Three-dimensional microfabrication with two-photon-absorbed photopolymerization," Opt. Lett. **22**(2), 132–134 (1997).
27. M. Vaezi, H. Seitz, and S. Yang, "A review on 3d micro-additive manufacturing technologies," Int. J. Adv. Manuf. Technol. **67**(5-8), 1721–1754 (2013).
28. S. K. Seol, D. Kim, S. Lee, J. H. Kim, W. S. Chang, and J. T. Kim, "Electrodeposition-based 3d printing of metallic microarchitectures with controlled internal structures," Small **11**(32), 3896–3902 (2015).
29. D. Momotenko, A. Page, M. Adobes-Vidal, and P. R. Unwin, "Write-read 3d patterning with a dual-channel nanopipette," ACS Nano **10**(9), 8871–8878 (2016).
30. L. Hirt, S. Ihle, Z. Pan, L. Dorwling-Carter, A. Reiser, J. M. Wheeler, R. Spolenak, J. Vörös, and T. Zambelli, "Template-free 3d microprinting of metals using a force-controlled nanopipette for layer-by-layer electrodeposition," Adv. Mater. **28**(12), 2311–2315 (2016).
31. V. F. Paz, M. Emons, K. Obata, A. Ovsianikov, S. Peterhänsel, K. Frenner, C. Reinhardt, B. Chichkov, U. Morgner, and W. Osten, "Development of functional sub-100 nm structures with 3d two-photon polymerization technique and optical methods for characterization," J. Laser Appl. **24**(4), 042004 (2012).
32. S. Maruo, A. Takaura, and Y. Saito, "Optically driven micropump with a twin spiral microrotor," Opt. Express **17**(21), 18525–18532 (2009).
33. A. Boltasseva and V. M. Shalaev, "Fabrication of optical negative-index metamaterials: Recent advances and outlook," Metamaterials (Amst.) **2**(1), 1–17 (2008).
34. A. Ovsianikov, S. Schlie, A. Ngezahayo, A. Haverich, and B. N. Chichkov, "Two-photon polymerization technique for microfabrication of cad-designed 3d scaffolds from commercially available photosensitive materials," J. Tissue Eng. Regen. Med. **1**(6), 443–449 (2007).
35. R. Guo, S. Xiao, X. Zhai, J. Li, A. Xia, and W. Huang, "Micro lens fabrication by means of femtosecond two photon photopolymerization," Opt. Express **14**(2), 810–816 (2006).
36. K. A. Abrashitova, D. N. Gulkin, N. G. Kokareva, K. R. Safronov, A. S. Chizhov, A. A. Ezhov, V. O. Bessonov, and A. A. Fedyanin, "Nonlinear polymer/quantum dots nanocomposite for two-photon nanolithography of photonic devices," Proc. SPIE **10115**, 101150 (2017).
37. Excillium microfocus Metal Jet X-ray source - *http://www.excillum.com/technology/metal-jet-technology.html*
38. F. Seiboth, A. Schropp, M. Scholz, F. Wittwer, C. Rödel, M. Wünsche, T. Ullsperger, S. Nolte, J. Rahomäki, K. Parfeniukas, S. Giakoumidis, U. Vogt, U. Wagner, C. Rau, U. Boesenberg, J. Garrevoet, G. Falkenberg, E. C. Galtier, H. Ja Lee, B. Nagler, and C. G. Schroer, "Perfect x-ray focusing via fitting corrective glasses to aberrated optics," Nat. Commun. **8**, 14623 (2017).
39. V. Nazmov, E. Reznikova, J. Mohr, A. Snigirev, I. Snigireva, S. Achenbach, and V. Saile, "Fabrication and preliminary testing of X-ray lenses in thick SU-8 resist layers," Microsyst. Technol. **10**(10), 716–721 (2004).
40. V. Nazmov, J. Mohr, H. Vogt, R. Simon, and S. Diabaté, "Multi-field x-ray microscope based on array of refractive lenses," J. Micromech. Microeng. **24**(7), 075005 (2014).

Optics EXPRESS

1. Introduction

X-ray refractive optics has been intensively developed within the last years. Since firstly introduced in 1996 as a drilled holes [1] in bulk aluminum, they have been realized in a wide spectrum of designs - in one [2] and two dimensions [3] with spherical [1], parabolic [4] or kinoform profile [5]. Reliability, compactness and ease of use accompanied by excellent focusing performance has made them very popular on the 3rd generation of X-Ray sources. Fabricated from materials with high refractive index such as Al, Be, C, Ni or Si they are capable of focusing high-energy radiation down to micro- and nano- scales thus fulfilling almost every task arising in modern synchrotron beamlines: long-focus lenses perform beam transport and energy filtering of the high-heat radiation at the front end [6–8], while two-dimensional lenses in X-ray transfocators [9, 10] act as secondary focusing, imaging and microscopy devices.

If refer to X-ray microscopy, the versatility of refractive optics allowed to integrate the observation of diffraction patterns [11, 12] and real-space images [13–15] within the one experimental setup. Moreover, dark-field X-ray microscopy was also recently realized [16]. However, the best achievable resolution of Be lenses is in the order of 100 nm [17] and it is mainly influenced by the inner material – polycrystalline beryllium introduces parasitic scattering - speckles and distortions - to the transmitted wave front. Another limit is the diffraction-limited resolution that is determined by a numerical aperture (*NA)* which needs to be maximal. Numerical aperture is in turn connected to the lens effective aperture, D_{eff}, which is identical to the physical aperture *2R* for visible light and glass lenses. As the refractive lenses are concerned, their effective aperture is smaller than *2R* due to the absorption in a lens material and this is a determining factor of the diffraction-limited resolution [18]. The effective aperture scales with the square root of the focal length, which is $F = R/2Nd$, where R is the radius of curvature of one parabolic surface, N is the number of double concave elements in the lens, d is the decrement of the refraction index. It is clear that a smaller radius of the parabola provides for a shorter focal distance and allows to achieve higher resolution yet approaching diffraction limit. In contrast with beryllium lenses, the existing manufacturing technology does not allow to produce lenses with a radius smaller than 50 μm.

In connection with all the limitations discussed above, silicon microfabrication technology was applied to reduce the radius of lenses. Silicon one-dimensional nano-lenses [19] have the smallest radii of few microns and are currently able to execute focusing down to 50 nm [20] with the theoretical limit of 2 nm [21]. However, silicon planar lenses have a major drawback - their one-dimensional profile makes it impossible to perform two-dimensional imaging of nano-objects. Even with a perfectly aligned cross-geometry lenses, the presence of aberrations is simply inevitable.

Consequently, in order to fabricate the small-radius lenses without parasitic X-ray scattering, we decided to turn to alternative methods of manufacturing from amorphous polymer materials. At this point, additive manufacturing (or 3D printing) is the most promising approach. It suggests creating the three-dimensional objects (i.e. lenses) by adding material layer-upon-layer under a computer control. Additive technologies can be based on different physical phenomenon such as laser [22] or ion/electron beam [23] induced deposition, photo reduction [24], one- [25] or two-photon [26] absorption induced polymerization, sintering or melting [27], electrodeposition [28–30]. During the last decades with huge advances in technology the resolution of many additive manufacturing methods has been downscaled to sub-microns.

One of the most elaborate methods is the two-photon absorption induced polymerization lithography, which was introduced for the first time as far as in 1996 [26]. It is a simple, reliable and relatively cheap method with sub-100 nm feature size [31] and a wide spectrum of processed materials. 2PP has made it possible to manufacture unique 3D structures, which could not be realized by any other technique. This has revolutionized many fields including microfluidics [32], metamaterials [33], biomedical science [34], optics [35] etc.

Optics EXPRESS

In the present paper, we introduce 2D parabolic X-ray refractive nano-lenses that were fabricated by 2PP lithography from amorphous polymer for the first time. We also test their optical performance in tests at the micro-focus X-ray laboratory source.

2. Lenses

Two photon polymerization lithography is based on polymer solidification by means of two photon absorption process - the simultaneous absorption of two photons, equivalent to the absorption of one photon with double frequency. Nonlinear character of absorption results in transparency of the out-of-focus polymer material, while the presence of polymerization threshold reduces resolution far below the diffraction limit. Together this results in unprecedented geometrical freedom allowing one to print very complex designs including overhanging and self-intersecting structures inaccessible by conventional methods.

3D printing process starts from 3D computer-aided-design (CAD) model in triangulated STL file format. The model is sliced into layers by special software called slicer resulting in contours of each layer. The same software with motion trajectories of printing unit then fills these contours. The latter are defined by various processing parameters including layer height, hatch distance (XY distance between adjacent lines), scanning speed, movement direction of printing unit and printing order, printing patterns etc. Tightly focused laser beam follows the trajectories obtained from slicing procedure in layer-by-layer manner thus fabricating arbitrary 3D objects.

In our experiments, we used a home-built 2PP setup [36] (Fig. 1(a)). The radiation from the laser source (Ti:Sa femtosecond laser, 800 nm wavelength, 80 MHz repetition rate, 50 fs pulse duration) passed through the prism pulse precompressor (PPC) in order to compensate positive dispersion and maintain the pulse duration as short as possible. A system of half-wave plate in a motorized rotational stage (L/2), Glan-Taylor prism (GP1) and photodiode (PD) was used to control the power of radiation incident on the sample with the accuracy of tens of microwatts. Acoustooptic modulator (AOM) worked as a fast shutter and second Glan-Taylor prism (GP2) controlled the polarization of incident light. Laser beam was expanded by the telescope to completely cover the entrance aperture of focusing oil-immersion objective (Olympus, 100-x magnification, 1.4 NA) which tightly focused light into the sample. Fast steering mirror (FSM) and piezo stage (PS) moved the beam waist inside the resin with the accuracy of 1nm in a field of 60μm x 60μm in the plane of a sample (XY plane) and with a 5 nm accuracy on a 200 μm travel range along the optical axis (Z axis). The sample was mounted on a microscope table (MT) that provided long-distance travel in the sample surface plane XY with a travel range of 11.5 cm in X direction and 7.5 cm in Y direction and accuracy of 100 nm. CMOS camera (CAM) was used to measure and compensate sample tilt and to visualize the process of polymerization. The 2PP setup was completely automatic.

The exposition could be provided in two geometries: from down to up starting exposing from a cover glass and moving upwards into the resin or from up to down with the photoresist confined between two cover glasses starting from the top cover glass and moving downwards into the liquid resin. Since illumination through the solidified material may induce scattering and therefore beam defocusing or can possibly induce explosion of the material. Thus, the exposition geometry was restricted: it was necessary to provide the exposition from up to down with the photoresist confined between two cover glasses (in a cell, Fig. 1).

Optics EXPRESS

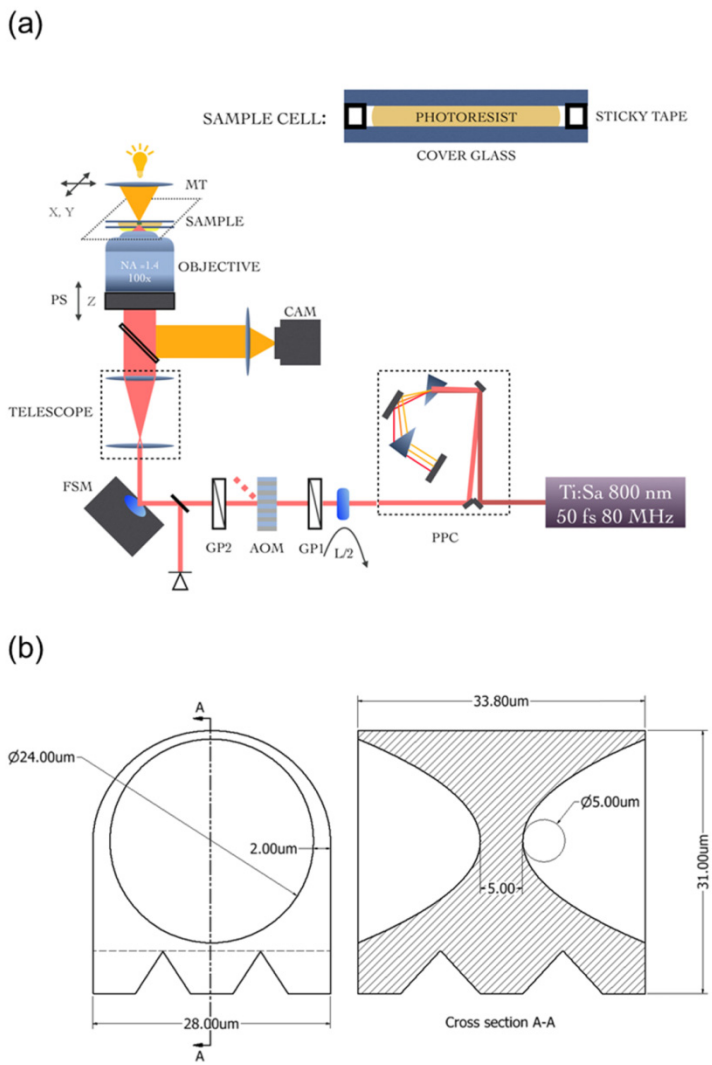

Fig. 1. The 2PP experimental setup (*a*) and model of polymer refractive lens (*b*).

The sample was prepared as follows: two cover glasses were washed with piranha solution (3 parts of concentrated sulfuric acid mixed with one part of 30% hydrogen peroxide solution) rinsed with deionized water (Direct-Q, Millipore) and dried in air. 4 pieces of sticky tape were stuck onto one of the cover glasses as spacer and the liquid photoresist (ORMOCOMP Microresist technology GmbH) was dropped between the tape pieces. The resulting cell was covered with the second cover glass. According to optical microscopy the thickness of the cell was 40 μm with repeatability of 10%. After exposure the sample was developed in the appropriate developer ORMODEV for 12 hours, rinsed with fresh developer and isopropanol and dried in air.

The most important processing conditions are the power, incident on the sample, the velocity of the laser beam waist movement, layer height and hatch distance (spacing between adjacent lines in Z and XY directions respectively). They determine the exposure dose for each voxel and thus the resolution and stiffness of the structure. First a preliminary experiment was conducted to optimize the power and the velocity. The best processing

Optics EXPRESS

parameters were determined to be 30 μm/s of beam velocity, 5.5mW of incident power and 200 nm layer height as well as hatch distance.

Applying the above-described technology we manufactured polymer refractive lenses with the following parameters [(Fig. 1(b)]. Radius of the curvature of a single parabolic surface, *R*, was 5 μm which is comparable with the radius of silicon nanolenses. Physical aperture was 24 μm in order to reduce the printing time. The distance between the parabola apexes was 5 μm. Thus, external dimensions of single lens were 28x34x29 μm^3. In order to lift lens optical axis above the substrate we placed the lens on 9 pillars with a height of 5 microns. Seven double concave individual lenses were placed by a distance of 200 μm from each other along the optical axis, forming a compound refractive lens (CRL). We would like to note that the proposed design was chosen in order to perform lens focusing at an X-ray laboratory source (see next section).

The 3D model of the CRL was converted to STL format and sliced by universal Simplify3D printing software. The layer height of 200 nm and equal hatch distance was chosen for lens fabrication. The filling algorithm was concentric with 3 external perimeters. After the slicing procedure the generated G-code was converted into the internal code of a 2PP setup custom software. To obtain a cross-sectional view of the lens, the additional half-lens model was also fabricated. SEM-images of fabricated CRL, single lens and cross-section view are presented in Fig. 2. Geometrical parameters of structures turned to slightly deviate from that of the model due to overexposure, hence the exposition process requires further optimization.

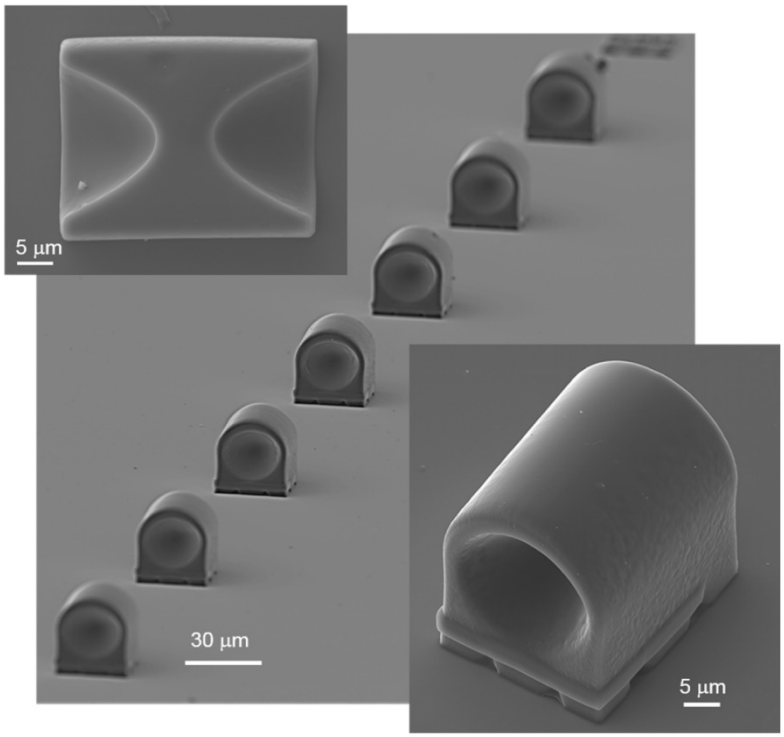

Fig. 2. SEM image of the fabricated polymer compound refractive lens. Upper insert shows the polymer lens in the cross-section. The insert in the bottom depicts individual refractive lens.

3. X-ray tests

Optical tests of lenses were performed at the Micro-optics test bench in X-ray optics laboratory of the Emmanuel Kant Baltic Federal University (Kaliningrad, Russia). The

Optics EXPRESS

scheme of the experimental set is shown in Fig. 3. In this setup, X-ray beam was produced by the Metal Jet (Excillium [37]) microfocus tube with a liquid-gallium jet as an anode, which has Ga K_α emission line at 9.25 keV. The source size was 10 µm in both vertical and horizontal directions. Radiation emitted from the source was collimated by vertical and horizontal slits with a size of 20 µm each, which were located at the distance of 11 cm from the source. A compound refractive lens (CRL) comprised of seven single lenses was mounted on a motorized stage enabling all necessary translation and rotation alignments. It was located at the distance L_1 of 26 cm from the source.

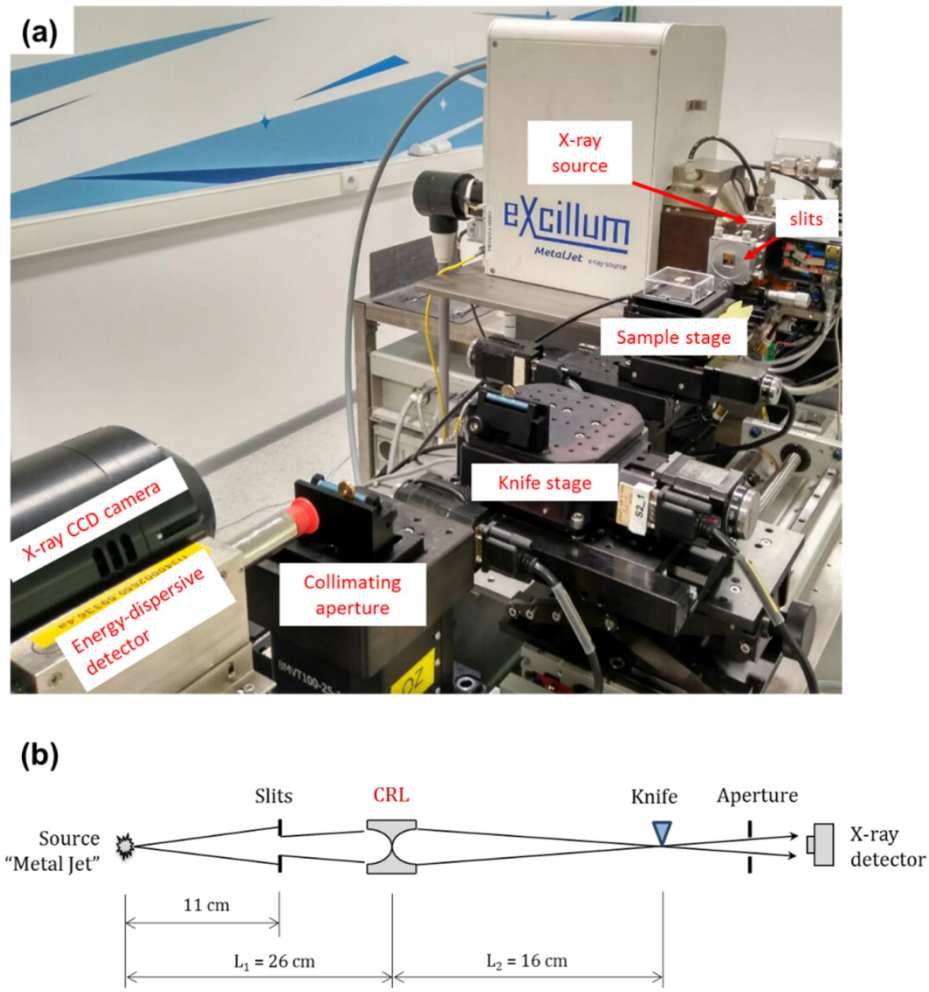

Fig. 3. Photograph (a) and layout (b) of the X-ray experiment.

CRL had the focal distance, F, of 10 cm at the radiation energy of 9.25 keV. For the source-to-lens distance, L_1, of 26 cm, according to the thin lens formula $1/F = 1/L_1 + 1/L_2$, imaging distance, L_2, was 16 cm. In this geometry, the source had to be projected with a demagnification $M = L_1 / L_2 = 1.6$. So, at the distance L_2 we expected to obtain the focal spot with the size of 6 µm.

All alignment procedures and preliminary measurements of focal spots were conducted using a high resolution X-ray CCD camera (Photonic Science, pixel size = 6.5 µm). To increase the accuracy of measurements we applied a knife-edge technique, where a tungsten wire with a diameter of 15 µm was placed on a motorized holder. It was scanning through the

Optics EXPRESS

beam while an energy-dispersive X-ray detector (X-123SDD, Amptek Technologies) was recording a transmitted integral intensity with the desired energy of 9.25 keV. Additionally, a Pt pinhole with a diameter of 30 µm was centred on the lens axis between the wire and the detector to shadow a radiation impinging onto the CRL outside of its aperture.

To find a focal spot of a minimal size, we performed several knife-edge scans moving the tungsten wire along the lens optical axis. The obtained values of focal spot sizes (full width at half maximum, FWHM) at different distances are shown in Fig. 4(a). We see that the minimal size appeared at the estimated earlier imaging distance L_2 of 16 cm. Figure 4(b) presents the vertical knife-edge scan in this location. The detected intensity as a function of wire position was differentiated and fitted by a Lorentzian function with the FWHM of 5 µm. The resulting beam profile is depicted by a red line. Taking into account the experimental error caused by the knife stage accuracy (± 1 µm), the size of the focused radiation is 5 ± 1 µm. This value clearly corresponds to the calculated value of 6 µm. Finally, by measuring X-ray absorption in the lens material we determined an effective aperture of the CRL to be 30 µm [18]. We should emphasize that this value was slightly larger than the lens physical aperture of 24 µm.

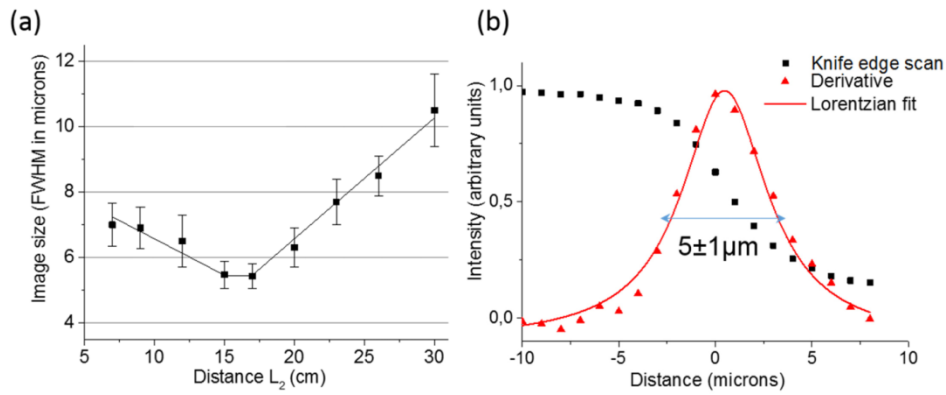

Fig. 4. Beam cross-sections measured at different distances along the lens optical axis (a) and the best knife-edge scan with the minimal size at the imaging distance L_2 = 16 cm (b).

4. Discussion and conclusion

The present study demonstrated that two-photon polymerization is a straightforward method for micro-fabrication of polymer refractive lenses with very small radius of curvature (5 µm). Their optical performance has been tested at the micro-focus X-ray laboratory source and the focal spot of 5 µm was measured. Taking into account that it was only the first demonstration, we believe that the manufacturing technology can be substantially optimized. We claim that the curvature radius might be downscaled to 400 nm with the current configuration of our 2PP setup and set of polymer materials. Applying the sophisticated 2PP techniques like stimulated emission-depletion lithography or diffusion-assisted direct laser writing, one can reduce this value even more. This technology may also be used for creating the X-ray phase correctors or beam-shaping elements [38].

It is obvious that the radiation damage of polymer lenses should be studied in greater detail in the nearest future. Currently ORMOCOMP photoresist was used for lens manufacturing and it is likely that it can be easily damaged in high-heat powerful beams. By implementing more chemically stable materials like SU-8 or lately introduced SZ-2080, heat-load performance of our lenses can be substantially improved. It is known that SU-8 lenses are widely used at some synchrotrons [39,40].

If refer to lens applications in X-ray microscopy and nano-probe techniques, a small radius can enhance numerical aperture and, therefore, the diffraction-limited resolution of the lens. Likewise, polymer lenses are amorphous and do not produce speckles as opposed to

Optics EXPRESS

refractive lenses from polycrystalline materials. Polymer is free of X-ray diffuse scattering from the grain boundaries, voids, inclusions and other scattering centres that reduce the amount of radiation in the focal spot. In addition, small and cheap plastic lenses may form very light and compact lens micro-objectives. This is particularly crucial for dark-field X-ray microscopy and is a considerable advantage in comparison with bulky and expensive beryllium lenses that are normally used in frames. Finally, due to the micron size, plastic lenses could be integrated into the same holder with a sample of interest.

Funding

Ministry of Education and Science of the Russian Federation grants contracts N° 14.W03.31.0008 and Nº 14.Y26.31.0002.

Acknowledgement

The manufacturing of polymer lenses was supported by grant contract N° 14.W03.31.0008, design and X-ray tests were performed by support of grant contract Nº 14.Y26.31.0002.